Science Advances
AAAS

Supplementary Materials for

Fetal hypoplastic lungs have multilineage inflammation that is reversed by amniotic fluid stem cell extracellular vesicle treatment

Lina Antounians *et al.*

Corresponding author: Augusto Zani, augusto.zani@sickkids.ca

Sci. Adv. **10**, eadn5405 (2024)
DOI: 10.1126/sciadv.adn5405

The PDF file includes:

Other Supplementary Material for this manuscript includes the following:

Supplementary Text

In vivo AFSC-EV administration routes

Pulmonary hypoplasia was induced in rat fetuses as described (*68-70*) with nitrofen (2,4-Dichloro-1-(4-nitrophenoxy)benzene) administration to dams by oral gavage on embryonic (E) 9.5. Three routes of administration were used to administer AFSC-EVs in vivo in rats 1) intra-tracheal: dams were anesthetized at E18.5, uterine horns were exposed through a midline laparotomy, and the head of the fetus was exposed through a prolene 6.0 purse string suture. The fetal trachea was dissected and intra-tracheal injection of 5 μL of AFSC-EVs or saline was conducted with a 30G needle to reach fetal lungs as in (*71-73*). The fetus was then returned to the amniotic sac and the purse string suture was closed. 2) intra-amniotic: dams were anesthetized at E18.5, a timepoint with ~40 fetal breathing movements/hour in rats (*74*), uterine horns were exposed through a midline laparotomy, and intra-amniotic injections of 100 μL of AFSC-EVs or saline were conducted randomly with a 30G needle, away from the body but close to the face of the fetus. No sutures were required, and sacs were returned into the dam. 3) maternal intra-venous: dams were anesthetized at E18.5, tail vein was identified and 100 μL of AFSC-EVs or saline were injected with a 25G needle. Samples were harvested at E21.5 for all three routes of administration and CDH presence was confirmed. To remove red blood cells, the lungs were perfused with saline, and the left lungs from CDH+ were harvested. The left lung was divided into four equal sized pieces, and the left lower lobe was reserved for snRNA-seq in selected samples. The rest of the pieces were immediately frozen and stored at -80°C or placed in 4% paraformaldehyde for fixation.

RNA expression

Harvested fetal lungs were frozen at -80 °C until analysis. Total RNA was isolated using Trizol reagent following supplier recommended protocols. Purified RNA was quantified using a NanoDrop™ spectrophotometer and cDNA synthesis was performed with 500 ng quantified RNA (superscript VILO cDNA synthesis kit). qPCR experiments were conducted with SYBR™ Green Master Mix for 45 cycles (denaturation: 95 °C, annealing: 58 °C, extension: 72 °C) using the primer sequences reported in table S7. Melt curve plots were used to determine target specificity of the primers. ΔΔCT method was used to determine normalized relative gene expression.

Immunofluorescence

Fetal rat lungs were fixed using 4% paraformaldehyde for 18 hours, paraffin-embedded, sectioned into 4 μm slices, and stained with primary antibodies reported in table S8, as reported previously (*6*). A Leica SP8 lightning confocal microscope (Wetzlar, Germany) was used to image samples using the same laser power and exposure between conditions. For human autopsy samples, two independent researchers differentiated between red blood cells and macrophages to quantify $CD68^+$ cells.

Protein expression

Protein from fetal rat lungs was isolated by incubation with cell extraction buffer supplemented with protease inhibitors, and sonication for 3 cycles of 10 seconds each. 20 μg of purified protein from each sample, quantified using the Pierce Bradford Assay, was probed for SPC and PDPN (table S8). ß-Actin was used as a loading control.

In vivo AFSC-EV tracking

For tracking the location of AFSC-EVs following administration in vivo, a subset of experiments was conducted with either IA or IV injection of 100 μL of fluorescently labeled AFSC-EVs

(ExoGlow™-Vivo) at E18.5. Each dose was 250 µg protein equivalent of AFSC-EVs stained with 2 µL of ExoGlow™-Vivo Near IR EV Labeling Kit (784 nm excitation, 820 nm emission), as per manufacturer's instruction. At E21.5, the whole body of the fetus or individually harvested organs were imaged using the IVIS® Spectrum In Vivo Imaging System – PerkinElmer (CFI Facility, University of Toronto). Briefly, whole fetuses were covered in talc powder to ensure optimal contrast and imaged with 2D fluorescence and 3D bioluminescence systems. Individual organs were reconstructed and imaged with 2D fluorescence using automatic exposure within an optimal range for quantification, avoiding overexposure during image acquisition, as recommended by the manufacturer. Saline-injected fetuses served as control. IVIS system was calibrated using 2 µL of ExoGlow™-Vivo. 3D reconstructions were generated using Living Image Software (version 4.7).

Lung morphometry

For lung morphometry, fixed sections of lungs were paraffin-embedded, stained with hematoxylin and eosin, and analyzed for radial airspace count as we previously described (*6*, *9*) and as recommended by the American Thoracic Society (*75*).

Flow cytometry

Total cells from fetal lungs were obtained using the Miltenyi Lung Dissociation Kit. Cells were fixed with 4% paraformaldehyde at 37°C for 10 min and resuspended in an HBSS sorting buffer containing 1-2% FBS. Following permeabilization cells were stained first for extracellular targets ADGRE-1 and CD43, and then for CD68 using primary antibodies reported in table S8. Cells were acquired using the Gallios 10/3 Flow cytometer (Beckman Coulter) and data was analyzed with the Kaluza software suite (Beckman Coulter). Data is representative of $n \geq 3$ rat fetuses.

Single nucleus RNA-sequencing experiments

Nuclei were extracted from frozen lung tissue using Singulator TM 100 (S2 Genomics), with the following settings: nuclear reagent, S2; incubation temp, cold; mixing type, top; mixing speed, fastest; disruption type, default; disruption speed, medium. RNase inhibitor was added to the Singulator Cartridge to reach a final concentration of 0.2 U/µl. Nuclei collected from the Singulator was spun at 800 g, at 4 °C for 10 min. Supernatant was removed, following by resuspending nuclei in freshly made cold Wash and Resuspension Buffer (1X saline, 1% bovine serum albumin, 0.2 U/µl). The wash was repeated twice before proceeding into the 10X Genomics single-cell 3' v3.1 assay and processed as described by the protocol provided by 10X Genomics. Libraries construction and library sequencing were proceeded as described in the 10X Genomics protocol using NovaSeq 6000. FastQ files were obtained using Cell Ranger (10X Genomics, cellranger-6.0.0), aligned to the Rattus norvegicus version 6 genome, and quantified with Cell Ranger count function using default settings. Sequencing data is available online at NCBI GEO, GSE211914. Further downstream analysis was performed in R (version 4.0.2) and bioinformatics tool Seurat (version 4.0.3), with default settings unless specified otherwise. Data were analyzed either by replicate or by pooling reads by condition. Filtering of data was performed to remove cells with raw data was log normalized and scaled using default values. Variable features and principal components were then calculated using default values. Ribosomal genes were removed with pattern = "^Rp[sl][[:digit:]]|^Rplp[[:digit:]]|^Rpsa" from normalized data. UMAP dimensionality reductions were performed with default values. Batch effects were not evident in the dimensionality reductions, and therefore, the data was then analyzed as-is without further corrections. We used LungMAP, LungCellMap, Tabula Muris, and Human Protein Atlas annotations from mouse and human lungs to assign cell type identity based on gene expression enrichment of key marker genes (*18-22*). For each major cell type, we performed differential

expression analysis using bioinformatics tool Seurat with MAST method between different conditions (e.g., Control+saline vs CDH+saline). We used Benjamini Hochberg corrected p-values for assessing statistical significance. Genes with p-value < 0.05 were considered as differentially expressed. Ligand-receptor analysis was performed using CellChat (Version 1.1.3, *76*) with default parameters. Gene set enrichment analysis was conducted using g:Profiler (version 0.7.0, *77*) and Reactome (*78*). To further delineate the specific macrophage subtypes contained in cluster 1, 2 and 5, we used scPred, a validated machine-learning probability-based prediction method and trained the machine algorithm on single cell data from adult rat lungs (*79, 80*).

Inhibition studies of macrophage activation

We performed intra-amniotic injections of GW2580 (15mg/kg) in nitrofen-exposed fetuses at E18.5 as described above. Fetuses were harvested at E21.5 and assessed for presence of CDH. Lungs from fetuses with CDH were used for analysis of RAC, as described above.

In vitro assay for macrophage activation

RAW264.7 cells were seeded onto a 6-well tissue culture plate (300,000 cells) and grown in DMEM/F12 + 10% FBS + 1% Penicillin/Streptomycin using culture media for 18 hours. The following day, differentiation medium (DMEM/F12 + 10% FBS + 1 ng/mL LPS + 1% Penicillin/Streptomycin) was added to stimulate RAW264.7 cells towards a pro-inflammatory phenotype for 24 hours. Following stimulation, 10% v/v of AFSC-EVs was added to the culture medium (50 µL of rat AFSC-EVs in 450 µL of DMEM/F12 + 10% FBS + 1% Penicillin/Streptomycin) for an additional 24 hours. RNA was extracted, quantified, and analyzed using ΔΔCT method relative to normalized gene expression, as described above, for *TNFa* and *Lcn2*.

miRNA-mRNA regulatory network analysis

It is well known that lung developmental processes are regulated at least in part by multiple miRNAs (*10*), whose expression is missing or dysregulated in experimental and human CDH lungs, as shown by several studies (*6, 11, 81-91*). Our previously published dataset of AFSC-EV miRNA cargo (*6*) was used to interrogate possible regulatory networks that were downregulated following AFSC-EV administration. We used miRNAs that were overexpressed in AFSC-EV cargo compared to another source of EVs from mesenchymal stromal/stem cells (*6*, data available in ArrayExpress E-MTAB-8921). Significantly downregulated genes in CDH+AFSC-EVs vs. CDH+saline groups were considered targets of AFSC-EV cargo miRNA. MultiMiR (v1.16.0, *92*) was used to link miRNAs from predicted and validated databases (miRecords, miRTarBase, TarBase) with targets. miRNA-mRNA pairs were visualized and shown as an interaction network generated using Cytoscape (3.8.2, *93*).

Comparison with EVs from other sources

In the context of other stem cell sources of EVs, we assessed mesenchymal stromal cells (MSCs) and HEK293 cells, an immortalized human embryonic kidney cell line.

MSC-EVs were chosen as they have been employed in a clinical trial for acute respiratory distress syndrome (ARDS) and were shown be safe and efficacious in restoring oxygenation, downregulating cytokine levels, and restoring immunity (*49*). Moreover, there has been ample evidence that stem cell-derived EVs have a beneficial effect also in premature lungs in several experimental studies (*94-101*). In these studies, MSC-EVs administered to different models of experimental BPD showed improvement in lung function, reversal of lung vascular remodeling and fibrosis, and attenuation of lung inflammation. MSC-EV beneficial effects to BPD lungs were found to be due to the epigenetic and phenotypic reprogramming of myeloid cells and modulation

of lung macrophage phenotype (*99, 102*). While we had previously shown that MSC-EV administration partially promoted epithelial cell homeostasis and differentiation in CDH lungs, we did not observe an improvement in several biological pathways and key phenotypic aspects of lung development, such as branching morphogenesis and alveolarization (*6, 8*). Conversely, we found that AFSC-EVs were a better candidate than MSC-EVs for reversing key features of pulmonary hypoplasia in CDH, likely due to their RNA cargo that was enriched with miRNAs responsible for lung developmental processes at a comparative analysis (*6*).

We also tested HEK293 cells as a non-stem cell source of EVs. Using the same methodology for isolation, characterization, and intra-amniotic administration as reported for AFSC-EVS, we observed that CDH fetal lungs treated with HEK293 cell-derived EVs did not have improvement in lung growth or maturation (fig. S8).

Statistical analysis

All statistical analyses were produced using GraphPad Prism® software version 6.0. Differential gene expression analysis was conducted using BioConducter R (3.15) package MAST (1.22.0) between two conditions, with adjusted p-value <0.05 and $\log_2$(fold change) $> |0.5|$ considered as significant for snRNA-seq experiments.

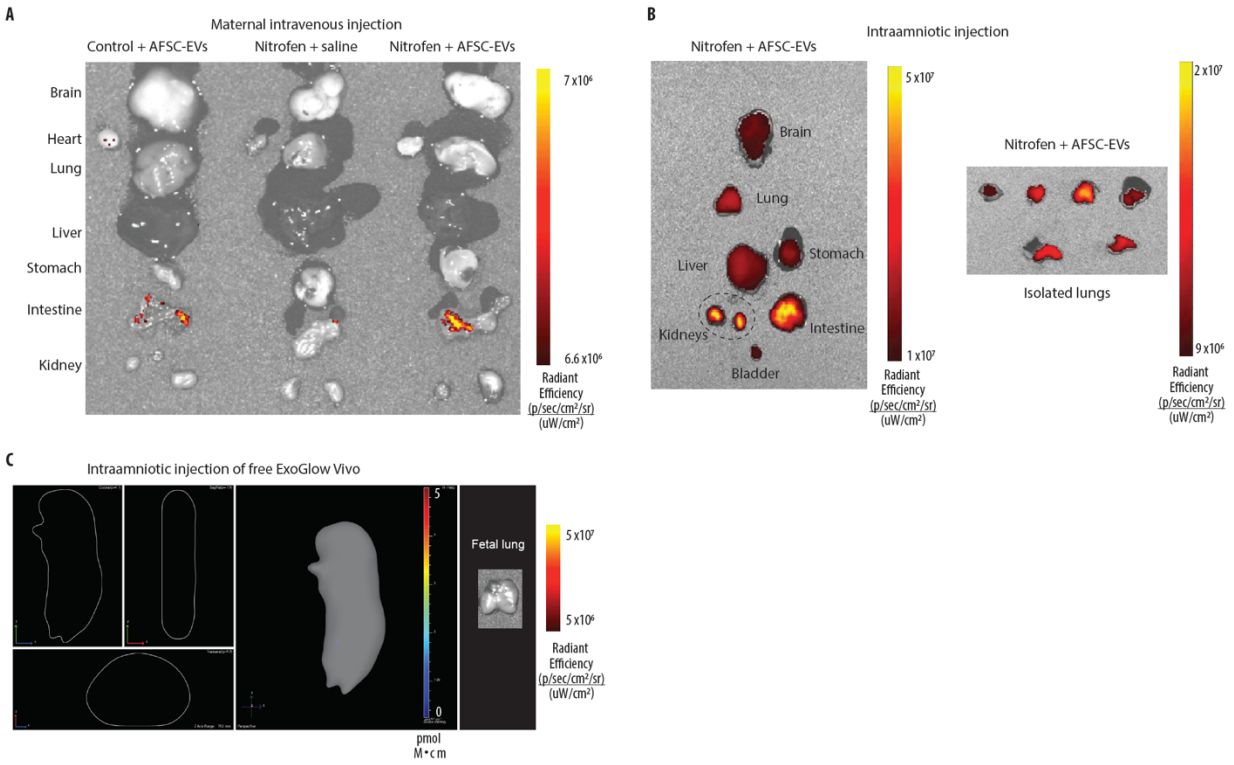

Fig. S1. In vivo effects on individual fetal organs. (**A**) Three representative 2-dimensional bioluminescence IVIS images of organs harvested from embryonic day E21.5 fetal rats following maternal intravenous injection of ExoGlowVivo-stained AFSC-EVs in control pups (left), or pups exposed to nitrofen and treated with AFSC-EVs (right), compared to nitrofen-exposed pups that received saline alone (middle). Control+saline (n=3), Nitrofen+saline (n=3), Nitrofen+AFSC-EVs (n=3). (**B**) Representative bioluminescence IVIS image of a nitrofen-exposed fetus treated with ExoGlowVivo-stained AFSC-EVs via intra-amniotic injection. Left side indicates all organs (n=10 biological replicates), right side shows fetal lungs from six different biological replicates. (**C**) Representative IVIS Spectrum instrument cross-sectional images of negative control from 3D bioluminescence reconstructions of whole fetuses at E21.5 that received intra-amniotic injection of free ExoGlowVivo-stained saline (n=3) at E18.5. Scale bar shows background-corrected

fluorescence in pmol M-1 cm-1. Representative 2D optical image of a dissected fetal lung from the same condition (right, n=4).

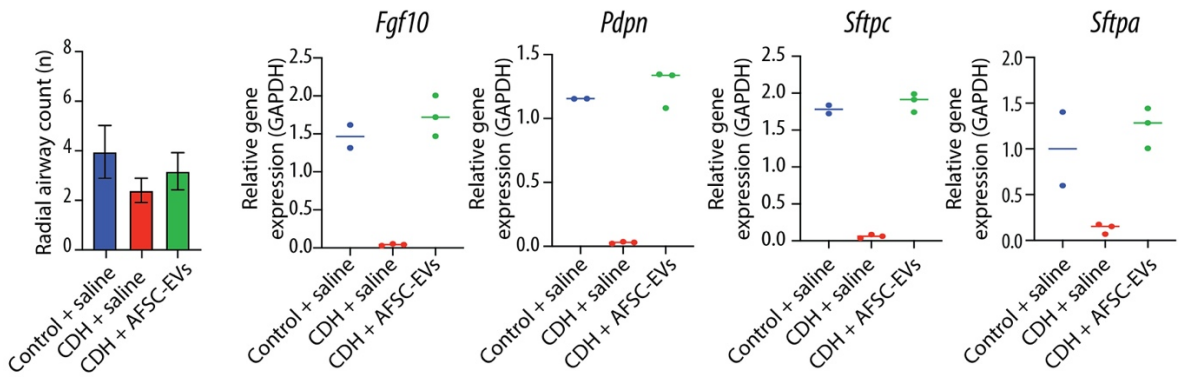

Fig. S2. Selection criteria for single nucleus RNA sequencing experiments. Quantification of radial airspace count and gene expression differences in lung developmental markers from the three experimental groups. Control+saline (n=2), CDH+saline (n=3), and CDH+AFSC-EV (n=3).

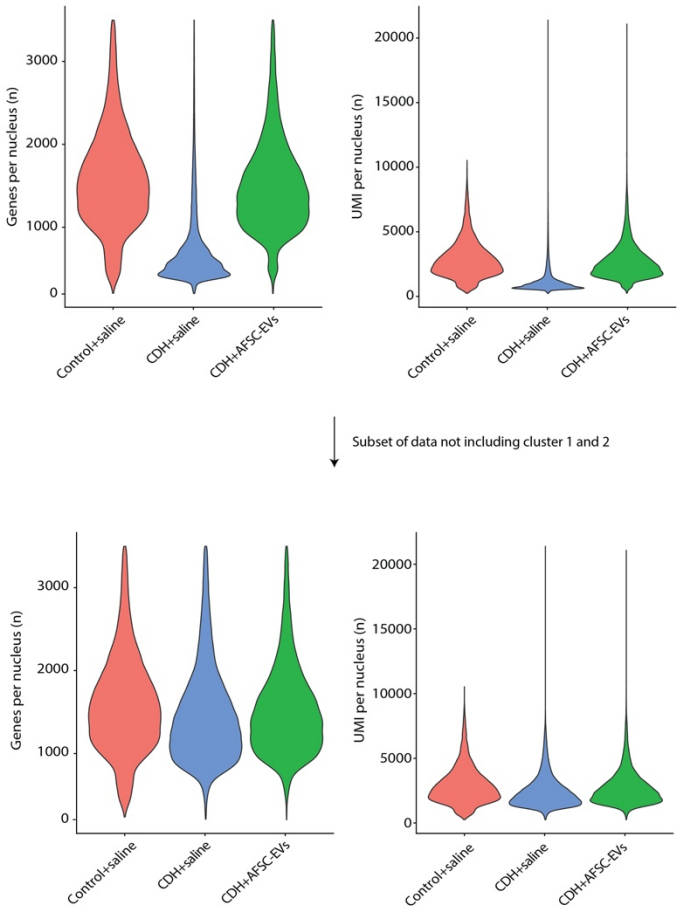

Fig. S3. Quality control metrics of single nucleus RNA-sequencing data. Plots of genes per nucleus and unique molecular identifiers (UMI) per nucleus in the final dataset (top) and subset of data that did not include cluster 1 and 2 from **Fig. 5F** (bottom).

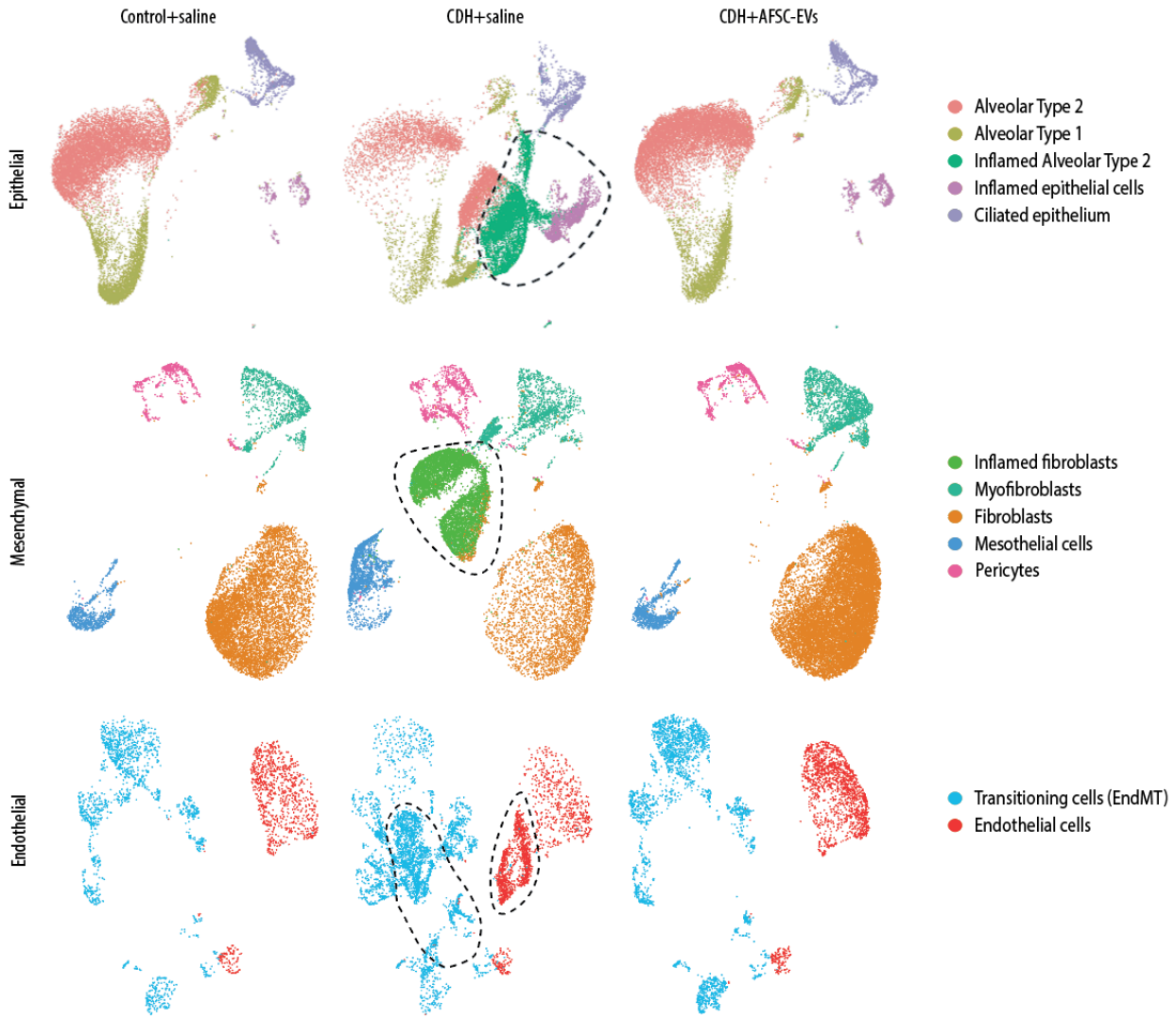

Fig. S4. UMAP depicting major cell types split by condition. Individual UMAPs of epithelial (top), mesenchymal (middle), and endothelial (bottom) cell types split by conditions: Control+saline (left), CDH+saline (middle), and CDH+AFSC-EVs (right). Colors indicate subgroups. Dotted lines outline the nuclei that are uniquely expressed in CDH+saline lungs.

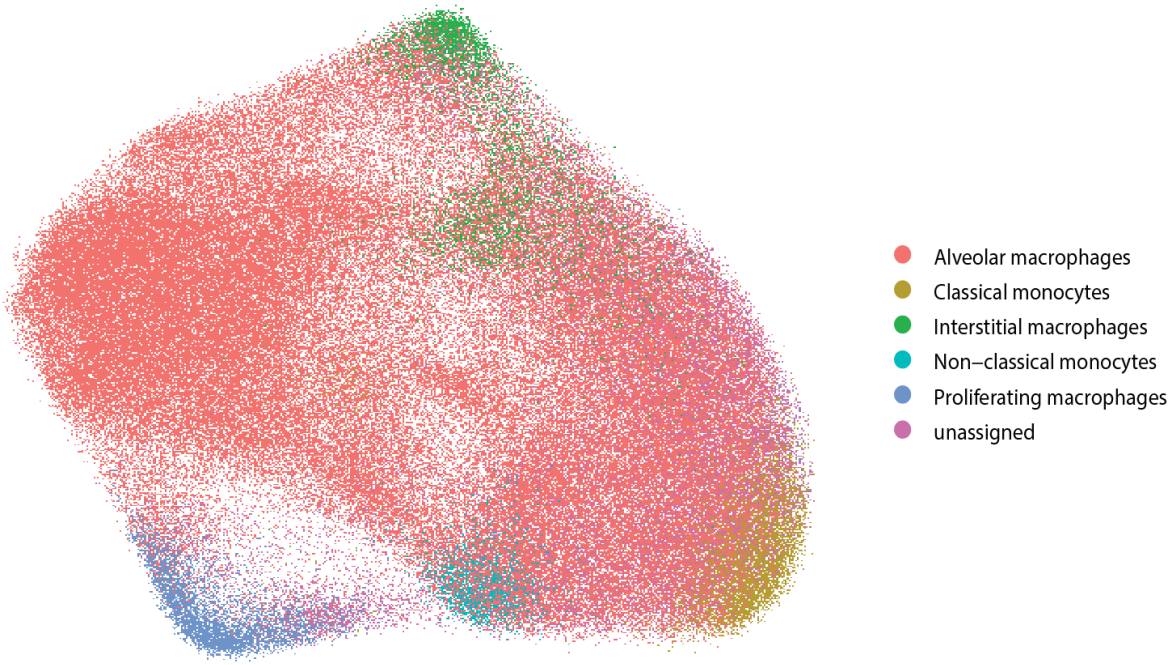

Fig. S5. Global UMAP of predicted subtypes in cluster 1 and 2. scPred tool was used to predict subtypes using machine learning on adult rat lung single cell data (*79, 80*). Colors indicate subgroups.

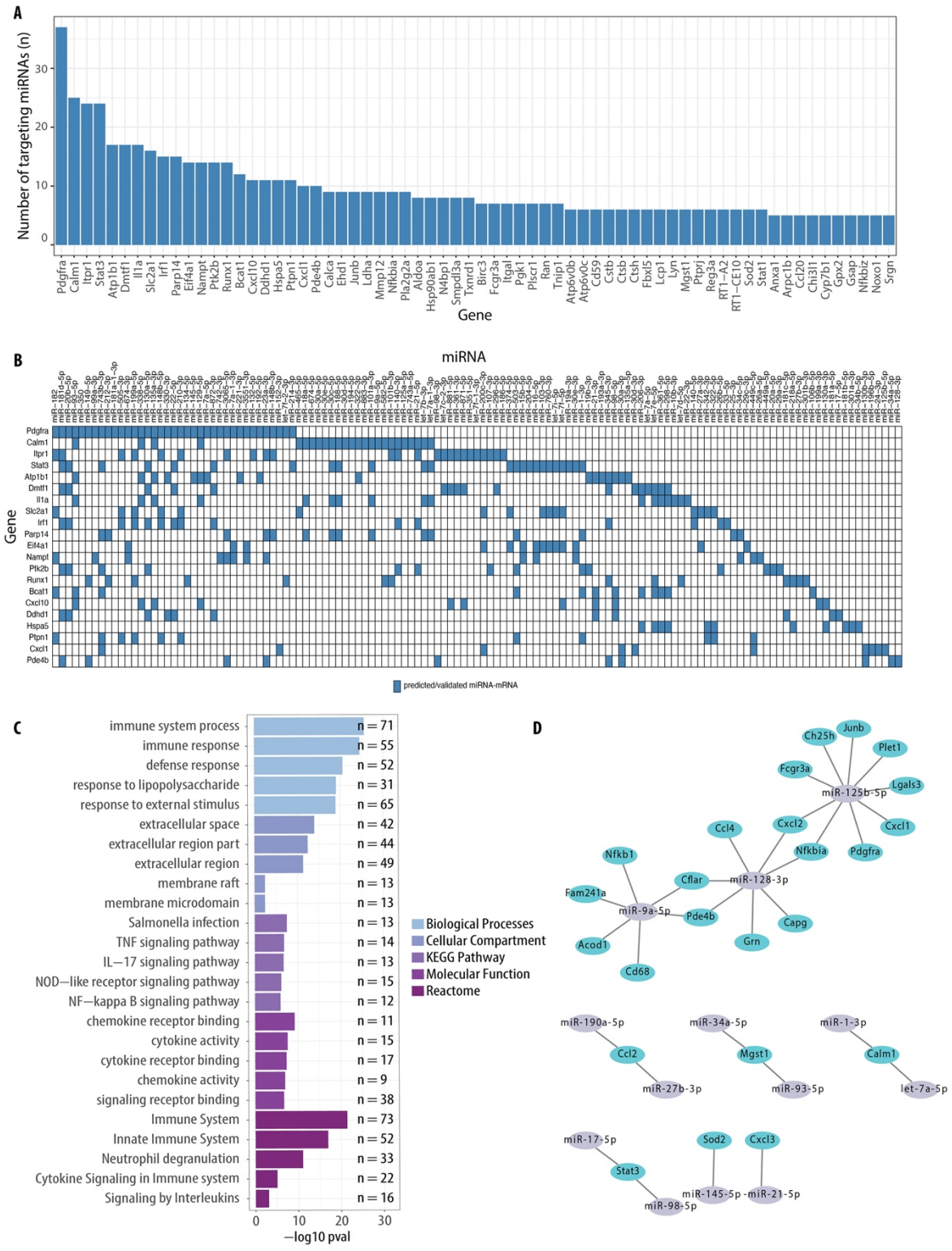

Fig. S6. Predicted miRNA-mRNA signaling pathways activated by AFSC-EVs. (**A**) Bar graph indicating number of miRNA-mRNA interactions (y-axis) between AFSC-EV cargo miRNAs and

down-regulated genes in CDH+AFSC-EV lungs (x-axis). Predicted miRNA-target interactions obtained from publicly available datasets (tarbase, MicroCosm, miRanda, miRDB, miRecords, miRTarBase). (**B**) Heatmap of specific AFSC-EV miRNAs (x-axis) and their redundant roles in downregulating genes in CDH+AFSC-EV lungs (y-axis). (**C**) Gene set enrichment analysis of the downregulated genes using g:Profiler. (**D**) Network of validated miRNA-mRNA pairs showing downregulated genes (blue nodes) and AFSC-EV miRNAs (purple nodes).

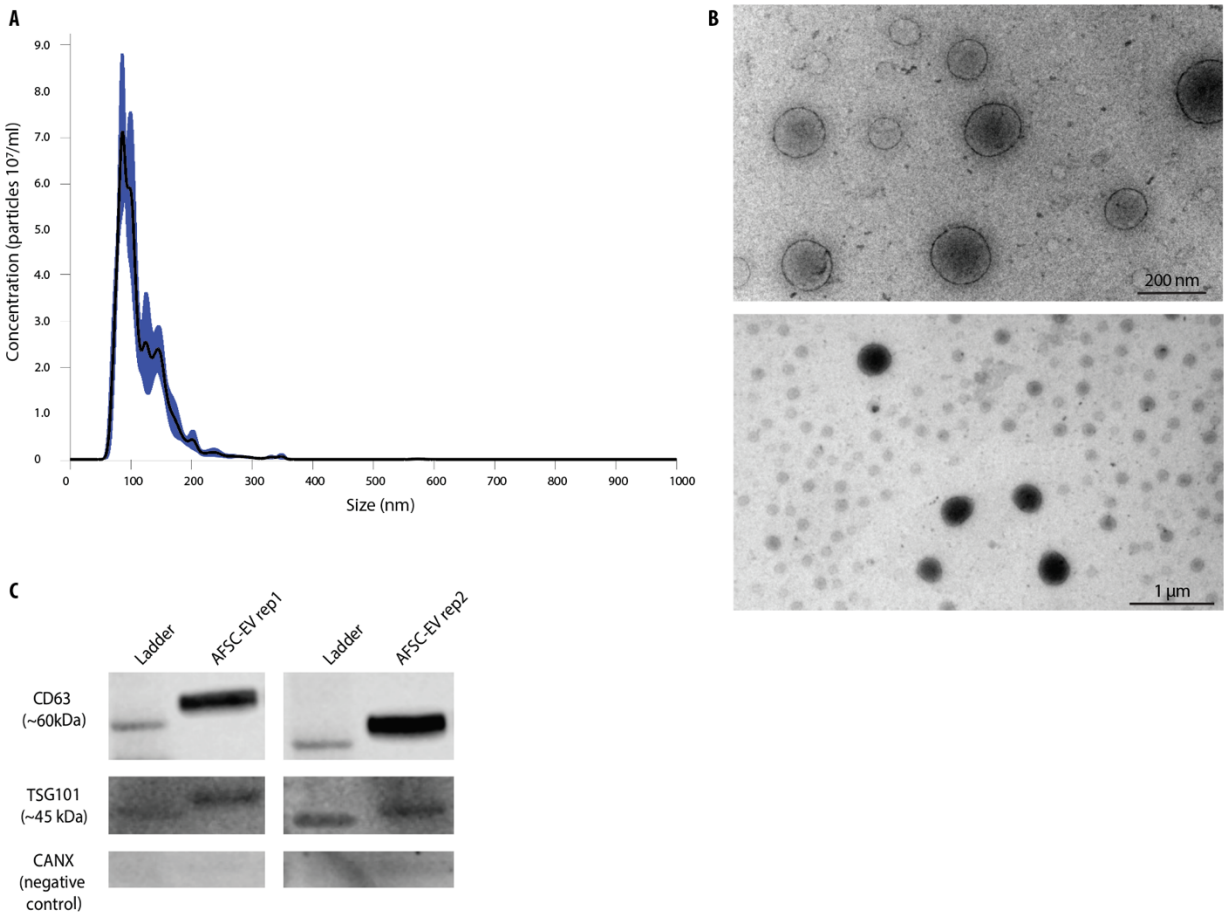

Fig. S7. Characterization of rat AFSC-EVs used in this study. (**A**) Representative plot of the average size distributions of AFSC-EVs using nanoparticle tracking analysis. Data are representative of five 30 second videos. (**B**) Representative photos of AFSC-EV morphology analyzed by transmission electron microscopy at two different magnifications (top, individual AFSC-EVs at near field; bottom population of AFSC-EVs at far field). Scale bar = 200 nm and 1 µm. (**C**) Expression of canonical markers of EVs (CD63 and TSG101) in a Western blotting experiment with two replicates of AFSC-EVs. AFSC-EV preparations are free of cellular debris as shown by lack of Calnexin (CANX) protein expression (negative control).

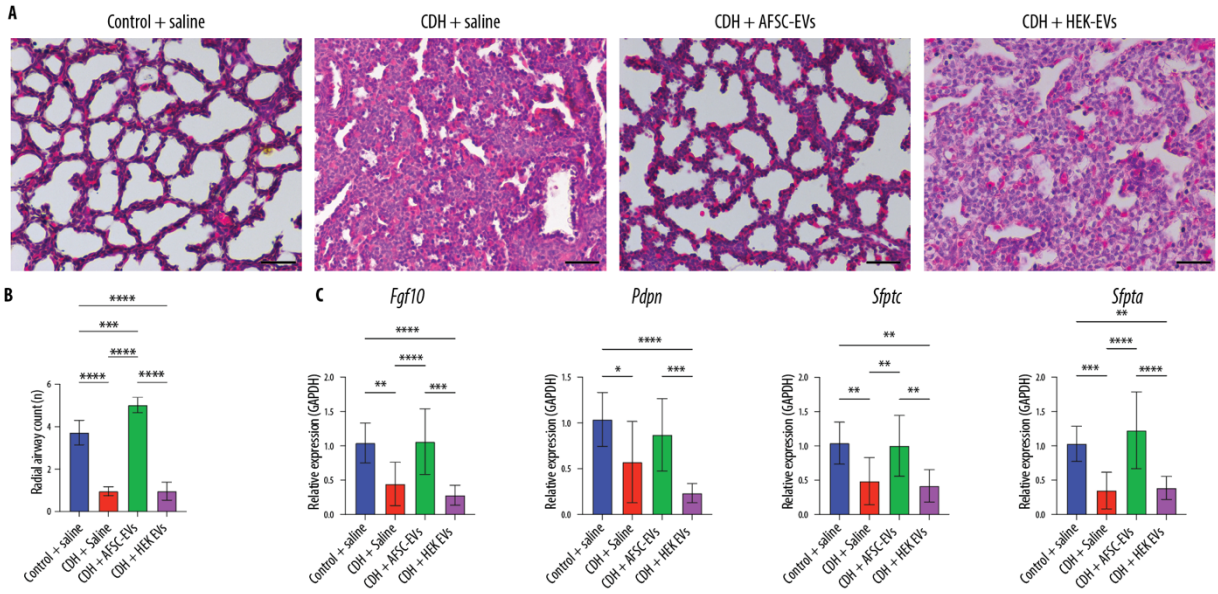

Fig. S8. Effects of HEK-derived EVs on hypoplastic nitrofen-exposed lungs. (**A**) Representative histology images (hematoxylin/eosin) of fetal lungs from Control+saline, CDH+saline, CDH+AFSC-EV, and CDH+HEK-EV fetuses. Scale bar = 50 µm. (**B**) Differences in number of alveoli (radial alveolar count, RAC) in Control+saline (n=5), CDH+saline (n=5), CDH+AFSC-EVs (n=5), and CDH+HEK-EVs (n=5) quantified in at least 5 fields per fetal lung. (**C**) Gene expression changes in lung developmental markers *Fgf10*, *Pdpn*, *Sftpc* and *Sftpa*. Control+saline (n=10), CDH+saline (n=10), CDH+AFSC-EVs (n=10), CDH+HEK-EVs (n=10).

Table S1: Number of nuclei in each cluster for snRNA-sequencing data analysis.

		number of nuclei per cluster		
Name	**cluster number**	**Control + saline**	**CDH + saline**	**CDH + AFSC-EVs**
Macrophage group 1	1	0	91109	0
Macrophage group 2	2	247	89187	739
Alveolar type 2	3	9721	5248	10578
Fibroblast	4	7045	3705	14069
Immune	5	1783	6610	4165
Alveolar type 1	6	4526	2459	3352
Inflamed fibroblast	7	6	6931	3
Inflamed alveolar type 2	8	13	6843	21
Myofibroblast	9	1150	1794	2185
EndMT	10	1575	3629	2386
Endothelial	11	974	1731	1614
Mesothelial	12	858	2114	1138
Ciliated epithelial	13	1417	1109	891
Inflamed epithelial	14	366	1864	880
Pericytes	15	630	1077	911

Table S2: Selected inflammatory genes that were upregulated in CDH fetal lungs compared to control.

Gene	Name	Function	Role during lung development and CDH (if known)	References
Visfatin	Nicotinamide phosphoribosyl-transferase	Peptide that enhances cell proliferation, biosynthesis of nicotinamide mono- and dinucleotide	Visfatin is a pro-inflammatory cytokine that potentiates TNFα and IL-6 production in human peripheral blood mononuclear cells and has been proposed as a biomarker for acute lung injury	(*103-106*)
Ptn	Pleiotrophin	Protein that has critical roles in cell growth and survival, cell migration, and angiogenesis	Ptn is a signaling molecule involved in fetal lung development and important for regulation of stem cell phenotype	(*107, 108*)
Lcn2	Lipocalin-2	Protein involved in the transport of small hydrophobic molecules such as lipids, steroid hormones and retinoids	Acute-phase protein involved in the immune response to lung inflammation.	(*109*)
Il1b	Interleukin 1b	Cytokine that is a mediator of the inflammatory response, and is involved in a variety of cellular activities, including cell proliferation, differentiation, and apoptosis	Il1B is known to stimulate the immune response and cause disruption of lung morphogenesis.	(110, 111)

Table S3: Genes upregulated in fetal lungs following in vivo AFSC-EV administration.

Gene	Name	Function	Role during lung development and CDH (if known)	References
Calcrl	Calcitonin receptor-like	Receptor of adrenomedulin (AM), which plays a key role in endothelial growth and development. AM is ubiquitously expressed, including in blood vessels and lungs.	AM has potential anti-inflammatory, antioxidant, angiogenic, and vasodilatory properties in the lungs. AM was found to increase pulmonary angiogenesis and attenuate alveolar simplification and pulmonary hypertension in a rat model of hyperoxia-induced BPD.	(*112-114*)
c-Kit	Tyrosine-protein kinase KIT, CD117	Proto-oncogene that interacts with cell growth factors and plays a role in cell survival, multiplication, and differentiation.	In the lung, c-Kit is responsible for maintenance of normal alveolar architecture, regulation of epithelial cell clonal expansion, and vascular formation.	(*115, 116*)
Igf	Insulin-like growth factor	Protein-coding gene that is involved in mediating growth and development in many cells and tissues.	The Igf system plays a pivotal role in the development and differentiation of the fetal lung. IGF receptor type 1 and type 2 are downregulated in nitrofen-induced hypoplastic lungs.	(*117-121*)
Vegf	Vascular endothelial growth factor	Potent mitogenic and angiogenic factor that is responsible for differentiation and proliferation of endothelial cells during embryogenesis.	Vegf plays a key role in the development of the pulmonary capillary bed. Experimental studies have suggested that changes in the Vegf signaling pathway are associated with pulmonary hypoplasia in CDH.	(*122-125*)
Fgf	Fibroblast growth factor	Regulates a broad spectrum of biological functions, including cellular proliferation, survival, migration and differentiation.	Fgf signaling plays a key role for branching morphogenesis during lung development, injury, and repair.	(*126-129*)
Egf	Epidermal growth factor	Plays an important role in the growth, proliferation and differentiation of numerous cell types.	Egf enhances alveolar type II cell differentiation and stimulates surfactant protein A synthesis. Its receptor is found in the alveolar epithelium during differentiation, suggesting an important role for Egf during human fetal lung development. Exogenous EGF	(*130, 131*)

			improves lung growth in the nitrofen-induced CDH model.	
Gas	Growth arrest-specific protein 1	Protein-coding gene that plays a key role in processes related to proliferation, inflammation, tissue repair, and angiogenesis.	In the lung, Gas signaling has been shown to reduce alveolar inflammation and acute ischemia-reperfusion injury. Furthermore, Gas is a promising molecular marker for therapies of chronic thromboembolic pulmonary hypertension.	(*132, 133*)
Pros	Protein-S1 encoding gene	Vitamin-K-dependent plasma protein-coding gene with anticoagulant properties.	Pros1 signaling regulates lung cancer cell proliferation, migration, and angiogenesis.	(*134, 135*)
Sema3	Semaphorin 3A gene	Protein-coding gene with multifunctional roles in embryonic development, immune regulation, and vascularization.	Sema3a stimulates branching morphogenesis and cell proliferation.	(*10, 136*)
Nrg	Neuroregulin 1	Belongs to the EGF family and is involved in tissue development and maturation.	Nrg controls fetal lung maturation through mesenchymal-epithelial interactions. Nrg1 induces branching morphogenesis in the developing lung through a P13K signal pathway. CDH fetal lungs are associated with decreased NGR1 expression in the lamb model of CDH.	(*137-139*)
Csf	Colony stimulating factor 1	Protein-coding gene that controls the production, differentiation, and function of macrophages.	CSF1 has a pivotal role in fetal lung development, with regenerative effects through polarization of macrophages towards an M2 phenotype.	(*140*)

Table S4: Predicted cell types from cluster 1 and 2 of CDH+saline lungs

	number of nuclei	percentage
Alveolar macrophages	140382	77%
Classical monocytes	5879	3%
Interstitial macrophages	6511	4%
Non-classical monocytes	2287	1%
Proliferating macrophages	4942	3%
Unassigned	21281	12%

Table S5: Number of nuclei within each condition of predicted cell types from cluster 5 (immune cells).

Cell Subtypes	Control + saline	CDH + saline	CDH + AFSC-EVs
Alveolar macrophages	53	168	79
B cells	113	147	268
CD8 T cells	12	4	18
Classical monocytes	338	939	983
Conventional dendritic	35	48	99
ILC2	4	2	14
Interstitial macrophages	245	497	740
Mast cells	41	8	40
Naive T cells	384	161	518
Neutrophils	58	3506	182
NK cells 1	37	24	65
NK cells 2	16	10	41
Non-classical monocytes	25	161	72
Plasmacytoid dendritic	19	9	33
Proliferating macrophages	55	314	243
Proliferating T cells	33	42	98
Regulatory T cells	18	19	57
unassigned	297	551	615

Table S6: Details from human lung autopsy specimens used in this study.

Case #	CDH	Age (Gestational weeks)	Description
1	+	19	Left-sided CDH, pulmonary hypoplasia
2	+	20	Left-sided CDH, pulmonary hypoplasia
3	+	26	Absence of left diaphragm, pulmonary hypoplasia
4	+	27	Left-sided CDH, pulmonary hypoplasia, intrauterine growth restriction, stillborn
5	-	19	Elected termination of pregnancy
6	-	20	Elected termination of pregnancy
7	-	18.4	Elected termination of pregnancy
8	-	19	Elected termination of pregnancy

Table S7. Primer sequences used in this study for rat qPCR.

Target	Forward primer	Reverse primer
Fgf10	5'-AGCTGTTCTCCTTCACCAAGTA-3'	5'-ACTCCGATTTCCACTGATGTTA-3'
Pdpn	5'-CCTCCACTTGCCAGCAGTA-3'	5'-GCATGTGGTCCTCAATCATAAC-3'
Sftpc	5'-AACGCCTTCTCATCGTGGTT-3'	5'-GGCTTATAGGCGGTCAGGAG-3'
Sftpa	5'-AACGAGGCCATTGCAAGTATT-3'	5'-GAAGCCCCATCCAGGTAGT-3'
Tnfa	5'-GCCTCCCTCTCATCAGTTCTAT-3'	5'- TGGGTGAGGAGCACGTAGT-3'
Lcn2	5'-CGATGTACAGCACCATCTATGA-3'	5'- CATGGCGAACTGGTTGTAGT-3'
Gapdh	5'-AGTGCCAGCCTCGTCTCATA-3'	5'-GAGAAGGCAGCCCTGGTAAC-3'
Actb	5'-GGCTGTGCTGTCCCTGTATG-3'	5'-CCATCTCCTGCTCGAAGTCTA-3'

Table S8: Details of antibodies used in this study.

Target	Antibody	Company	Immunofluorescence concentration	Western blotting concentration
SPC	ab40879	Abcam	1:200	-
SPC	AB3786	EDM Millipore	-	1:500
PDPN	P5374	ThermoFisher	1:200	1:500
ß-actin	ab8226	Abcam	-	1:1000
CD68	ab283654	Abcam	1:100	-
pNFκB-p65 (Ser 536)	#3036	Cell signal	1:100	-
TNFα	sc-1350	Santa Cruz	1:200	-
CD63	EXOAB-CD63A-1	SBI	-	1:500
TSG101	sc78964	Santa Cruz	-	1:1000
Calnexin	ab22595	Abcam	-	1:1000

Movie S1. Representative 3-dimensional image of in vivo AFSC-EV tracking experiments for Control+AFSC-EVs.

Movie S2. Representative 3-dimensional image of in vivo AFSC-EV tracking experiments Nitrofen+AFSC-EVs.

Movie S3. Representative 3-dimensional image of in vivo AFSC-EV tracking experiments Nitrofen+saline (negative control).

Data file S1. Differentially expressed genes between Control+saline, CDH+saline, and CDH+AFSC-EVs by major cell type in fetal rat lungs.

Data file S2. Gene set enrichment analysis of differentially expressed genes between Control+saline vs. CDH+saline and CDH+saline vs. CDH+AFSC-EVs.

Data file S3. Unstained controls for flow cytometry. Flow cytometry analysis of unstained controls for ADGRE-1 (EMR-1), CD43, CD68 triple stain experiment. Panels are representative of $n \geq 3$ pups per group.

Data file S4. Gene set enrichment analysis of differentially expressed genes in CDH+saline lungs.

Data file S5. Data for Western blotting experiments.

REFERENCES AND NOTES

1. C. M. Cotten, Pulmonary hypoplasia. *Semin. Fetal Neonatal Med.* **22**, 250–255 (2017).

2. A. Zani, W. K. Chung, J. Deprest, M. T. Harting, T. Jancelewicz, S. M. Kunisaki, N. Patel, L. Antounians, P. S. Puligandla, R. Keijzer, Congenital diaphragmatic hernia. *Nat. Rev. Dis. Primers.* **8**, 37 (2022).

3. Global PaedSurg Research Collaboration, Mortality from gastrointestinal congenital anomalies at 264 hospitals in 74 low-income, middle-income, and high-income countries: A multicentre, international, prospective cohort study. *Lancet* **398**, 325–339 (2021).

4. C. Jeanty, S. M. Kunisaki, T. C. MacKenzie, Novel non-surgical prenatal approaches to treating congenital diaphragmatic hernia. *Semin. Fetal Neonatal Med.* **19**, 349–356 (2014).

5. R. L. Figueira, L. Antounians, E. Zani-Ruttenstock, K. Khalaj, A. Zani, Fetal lung regeneration using stem cell-derived extracellular vesicles: A new frontier for pulmonary hypoplasia secondary to congenital diaphragmatic hernia. *Prenat. Diagn.* **42**, 364–372 (2022).

6. L. Antounians, V. D. Catania, L. Montalva, B. D. Liu, H. Hou, C. Chan, A. C. Matei, A. Tzanetakis, B. Li, R. L. Figueira, K. M. da Costa, A. P. Wong, R. Mitchell, A. L. David, K. Patel, P. De Coppi, L. Sbragia, M. D. Wilson, J. Rossant, A. Zani, Fetal lung underdevelopment is rescued by administration of amniotic fluid stem cell extracellular vesicles in rodents. *Sci. Transl. Med.* **13**, eaax5941 (2021).

7. M. Yáñez-Mó, P. R. Siljander, Z. Andreu, A. B. Zavec, F. E. Borràs, E. I. Buzas, K. Buzas, E. Casal, F. Cappello, J. Carvalho, E. Colás, A. Cordeiro-da Silva, S. Fais, J. M. Falcon-Perez, I. M. Ghobrial, B. Giebel, M. Gimona, M. Graner, I. Gursel, M. Gursel, N. H. Heegaard, A. Hendrix, P. Kierulf, K. Kokubun, M. Kosanovic, V. Kralj-Iglic, E.-M. Krämer-Albers, S. Laitinen, C. Lässer, T. Lener, E. Ligeti, A. Linē, G. Lipps, A. Llorente, J. Lötvall, M. Manček-Keber, A. Marcilla, M. Mittelbrunn, I. Nazarenko, E. N. M. Nolte-‘t Hoen, T. A. Nyman, L. O'Driscoll, M. Olivan, C. Oliveira, É. Pállinger, H. A. Del Portillo, J. Reventós, M. Rigau, E. Rohde, M. Sammar, F. Sánchez-Madrid, N. Santarém, K. Schallmoser, M. S. Ostenfeld, W. Stoorvogel, R. Stukelj, S. G. Van der Grein, M. H. Vasconcelos, M. H. Wauben, O. De Wever, Biological

properties of extracellular vesicles and their physiological functions. *J. Extracell. Vesicles* **4**, 27066 (2015).

8. K. Khalaj, R. L. Figueira, L. Antounians, S. Gandhi, M. Wales, L. Montalva, G. Biouss, A. Zani, Treatment with amniotic fluid stem cell extracellular vesicles promotes fetal lung branching and cell differentiation at canalicular and saccular stages in experimental pulmonary hypoplasia secondary to congenital diaphragmatic hernia. *Stem Cells Transl. Med.* **11**, 1089–1102 (2022).

9. K. Khalaj, L. Antounians, R. L. Figueira, M. Post, A. Zani, Autophagy is impaired in fetal hypoplastic lungs and rescued by administration of amniotic fluid stem cell extracellular vesicles. *Am. J. Respir. Crit. Care Med.* **206**, 476–487 (2022).

10. A. Horowitz, M. Simons, Branching morphogenesis. *Circ. Res.* **103**, 784–795 (2008).

11. P. Pereira-Terra, J. A. Deprest, R. Kholdebarin, N. Khoshgoo, P. DeKoninck, A. A. Munck, J. Wang, F. Zhu, R. J. Rottier, B. M. Iwasiow, J. Correia-Pinto, D. Tibboel, M. Post, R. Keijzer, Unique tracheal fluid microRNA signature predicts response to FETO in patients with congenital diaphragmatic hernia. *Ann. Surg.* **262**, 1130–1140 (2015).

12. R. L. Figueira, N. Khoshgoo, F. Doktor, K. Khalaj, T. Islam, N. Moheimani, M. Blundell, L. Antounians, M. Post, A. Zani, Antenatal administration of extracellular vesicles derived from amniotic fluid stem cells improves lung function in neonatal rats with congenital diaphragmatic hernia. Journal of Pediatric Surgery 10.1016/j.jpedsurg.2024.02.029 (2024).

13. R. Ruano, J. L. Peiro, M. M. da Silva, J. A. Campos, E. Carreras, U. Tannuri, M. Zugaib, Early fetoscopic tracheal occlusion for extremely severe pulmonary hypoplasia in isolated congenital diaphragmatic hernia: Preliminary results. *Ultrasound Obstet. Gynecol.* **42**, 70–76 (2013).

14. J. A. Deprest, K. H. Nicolaides, A. Benachi, E. Gratacos, G. Ryan, N. Persico, H. Sago, A. Johnson, M. Wielgoś, C. Berg, B. van Calster, F. M. Russo, TOTAL Trial for Severe Hypoplasia Investigators, Randomized trial of fetal surgery for severe left diaphragmatic hernia. *N. Engl. J. Med.* **385**, 107–118 (2021).

15. M. Carlon, J. Toelen, A. Van der Perren, L. H. Vandenberghe, V. Reumers, L. Sbragia, R. Gijsbers, V. Baekelandt, U. Himmelreich, J. M. Wilson, J. Deprest, Z. Debyser, Efficient gene transfer into the mouse lung by fetal intratracheal injection of rAAV2/6.2. *Mol. Ther.* **18**, 2130–2138 (2010).

16. P. Klaritsch, S. Mayer, L. Sbragia, J. Toelen, X. Roubliova, P. Lewi, J. A. Deprest, Albumin as an adjunct to tracheal occlusion in fetal rats with congenital diaphragmatic hernia: A placebo-controlled study. *Am. J. Obstet. Gynecol.* **202** 198.e1–9 (2010).

17. L. Montalva, A. Zani, Assessment of the nitrofen model of congenital diaphragmatic hernia and of the dysregulated factors involved in pulmonary hypoplasia. *Pediatr. Surg. Int.* **35**, 41–61 (2019).

18. M. E. Ardini-Poleske, R. F. Clark, C. Ansong, J. P. Carson, R. A. Corley, G. H. Deutsch, J. S. Hagood, N. Kaminski, T. J. Mariani, S. S. Potter, G. S. Pryhuber, D. Warburton, J. A. Whitsett, S. M. Palmer, N. Ambalavanan, LungMAP: The molecular atlas of lung development program. *Am. J. Physiol. Lung Cell. Mol. Physiol.* **313**, L733-L740 (2017).

19. K. J. Travaglini, A. N. Nabhan, L. Penland, R. Sinha, A. Gillich, R. V. Sit, S. Chang, S. D. Conley, Y. Mori, J. Seita, G. J. Berry, J. B. Shrager, R. J. Metzger, C. S. Kuo, N. Neff, I. L. Weissman, S. R. Quake, M. A. Krasnow, A molecular cell atlas of the human lung from single-cell RNA sequencing. *Nature* **587**, 619–625 (2020).

20. M. Karlsson, C. Zhang, L. Méar, W. Zhong, A. Digre, B. Katona, E. Sjöstedt, L. Butler, J. Odeberg, P. Dusart, F. Edfors, P. Oksvold, K. von Feilitzen, M. Zwahlen, M. Arif, O. Altay, X. Li, M. Ozcan, A. Mardinoglu, L. Fagerberg, J. Mulder, Y. Luo, F. Ponten, M. Uhlén, C. Lindskog, A single-cell type transcriptomics map of human tissues. *Sci. Adv.* **7**, eabh2169 (2021).

21. B. Treutlein, D. G. Brownfield, A. R. Wu, N. F. Neff, G. L. Mantalas, F. H. Espinoza, T. J. Desai, M. A. Krasnow, S. R. Quake, Reconstructing lineage hierarchies of the distal lung epithelium using single-cell RNA-seq. *Nature* **509**, 371–375 (2014).

22. Tabula Muris Consortium, Single-cell transcriptomics of 20 mouse organs creates a Tabula Muris. *Nature* **562**, 367–372 (2018).

23. C. Pridans, K. M. Irvine, G. M. Davis, L. Lefevre, S. J. Bush, D. A. Hume, Transcriptomic analysis of rat macrophages. *Front. Immunol.* **11**, 594594 (2021).

24. J. G. Conway, B. McDonald, J. Parham, B. Keith, D. W. Rusnak, E. Shaw, M. Jansen, P. Lin, A. Payne, R. M. Crosby, J. H. Johnson, L. Frick, M. H. Lin, S. Depee, S. Tadepalli, B. Votta, I. James, K. Fuller, T. J. Chambers, F. C. Kull, S. D. Chamberlain, J. T. Hutchins, Inhibition of colony-stimulating-factor-1 signaling in vivo with the orally bioavailable cFMS kinase inhibitor GW2580. *Proc. Natl. Acad. Sci. U.S.A.* **102**, 16078–16083 (2005).

25. R. Wagner, G. M. Amonkar, W. Wang, J. E. Shui, K. Bankoti, W. Hei Tse, F. A. High, J. M. Zalieckas, T. L. Buchmiller, A. Zani, R. Keijzer, P. K. Donahoe, P. H. Lerou, X. Ai, A tracheal aspirate-derived airway basal cell model reveals a proinflammatory epithelial defect in congenital diaphragmatic hernia. *Am. J. Respir. Crit. Care Med.* **207**, 1214–1226 (2023).

26. B. M. Varisco, Nuclear factor-κB keeps basal cells undifferentiated in congenital diaphragmatic hernia. *Am. J. Respir. Crit. Care Med.* **207**, 1122–1123 (2023).

27. K. Ohshiro, E. Miyazaki, Y. Taira, P. Puri, Upregulated tumor necrosis factor-alpha gene expression in the hypoplastic lung in patients with congenital diaphragmatic hernia. *Pediatr. Surg. Int.* **14**, 21–24 (1998).

28. T. Schaible, M. Veit, J. Tautz, S. Kehl, K. Büsing, D. Monz, L. Gortner, E. Tutdibi, Serum cytokine levels in neonates with congenital diaphragmatic hernia. *Klin. Padiatr.* **223**, 414–418 (2011).

29. F. Kipfmueller, K. Heindel, A. Geipel, C. Berg, P. Bartmann, H. Reutter, A. Mueller, S. Holdenrieder, Expression of soluble receptor for advanced glycation end products is associated with disease severity in congenital diaphragmatic hernia. *Am. J. Physiol. Lung Cell. Mol. Physiol.* **316**, L1061-L1069 (2019).

30. R. Perry, J. Stein, G. Young, R. Ramanathan, I. Seri, L. Klee, P. Friedlich, Antithrombin III administration in neonates with congenital diaphragmatic hernia during the first three days of extracorporeal membrane oxygenation. *J. Pediatr. Surg.* **48**, 1837–1842 (2013).

31. M. Pavcnik-Arnol, B. Bonac, M. Groselj-Grenc, M. Derganc, Changes in serum procalcitonin, interleukin 6, interleukin 8 and C-reactive protein in neonates after surgery. *Eur. J. Pediatr. Surg.* **20**, 262–266 (2010).

32. S. Fleck, G. Bautista, S. M. Keating, T. H. Lee, R. L. Keller, A. J. Moon-Grady, K. Gonzales, P. J. Norris, M. P. Busch, C. J. Kim, R. Romero, H. Lee, D. Miniati, T. C. MacKenzie, Fetal production of growth factors and inflammatory mediators predicts pulmonary hypertension in congenital diaphragmatic hernia. *Pediatr. Res.* **74**, 290–298 (2013).

33. M. Okawada, H. Kobayashi, E. Tei, T. Okazaki, G. J. Lane, A. Yamataka, Serum monocyte chemotactic protein-1 levels in congenital diaphragmatic hernia. *Pediatr. Surg. Int.* **23**, 487–491 (2007).

34. K. Lingappan, O. O. Olutoye II, A. Cantu, M. E. Cantu Gutierrez, N. Cortes-Santiago, J. D. Hammond, J. Gilley, J. R. Quintero, H. Li, F. Polverino, J. P. Gleghorn, S. G. Keswani, Molecular insights using spatial transcriptomics of the distal lung in congenital diaphragmatic hernia. *Am. J. Physiol. Lung Cell. Mol. Physiol.* **325**, L477–L486 (2023).

35. J. H. Gosemann, F. Friedmacher, A. Hofmann, J. Zimmer, J. F. Kuebler, S. Rittinghausen, A. Suttkus, M. Lacher, L. Alvarez, N. Corcionivoschi, P. Puri, Prenatal treatment with rosiglitazone attenuates vascular remodeling and pulmonary monocyte influx in experimental congenital diaphragmatic hernia. *PLOS ONE* **13**, e0206975 (2018).

36. J. H. Gosemann, T. Doi, B. Kutasy, F. Friedmacher, J. Dingemann, P. Puri, Alterations of peroxisome proliferator-activated receptor γ and monocyte chemoattractant protein 1 gene expression in the nitrofen-induced hypoplastic lung. *J. Pediatr. Surg.* **47**, 847–851 (2012).

37. H. Shima, K. Ohshiro, Y. Taira, E. Miyazaki, T. Oue, P. Puri, Antenatal dexamethasone suppresses tumor necrosis factor-alpha expression in hypoplastic lung in nitrofen-induced diaphragmatic hernia in rats. *Pediatr. Res.* **46**, 633–637 (1999).

38. R. Wagner, P. Lieckfeldt, H. Piyadasa, M. Markel, J. Riedel, C. Stefanovici, N. Peukert, D. Patel, G. Derraugh, S. L. Min, J. H. Gosemann, J. Deprest, C. D. Pascoe, A. Tse, M. Lacher, N. Mookherjee, R. Keijzer, Proteomic profiling of hypoplastic lungs suggests an underlying inflammatory response in the pathogenesis of abnormal lung development in congenital diaphragmatic hernia. *Ann. Surg.* **278**, e411-e421 (2023).

39. F. Dylong, J. Riedel, G. M. Amonkar, N. Peukert, P. Lieckfeldt, K. Sturm, B. Höxter, W. H. Tse, Y. Miyake, M. Moormann, L. M. Bode, S. Mayer, R. Keijzer, M. Lacher, X. Ai, J. H. Gosemann, R. Wagner, Overactivated epithelial NF-κB disrupts lung development in congenital diaphragmatic hernia. *Am. J. Respir. Cell Mol. Biol.* **69**, 545–555 (2023).

40. J. L. Peiro, M. Oria, E. Aydin, R. Joshi, N. Cabanas, R. Schmidt, C. Schroeder, M. Marotta, B. M. Varisco, Proteomic profiling of tracheal fluid in an ovine model of congenital diaphragmatic hernia and fetal tracheal occlusion. *Am. J. Physiol. Lung Cell. Mol. Physiol.* **315**, L1028-L1041 (2018).

41. M. Guilliams, I. De Kleer, S. Henri, S. Post, L. Vanhoutte, S. De Prijck, K. Deswarte, B. Malissen, H. Hammad, B. N. Lambrecht, Alveolar macrophages develop from fetal monocytes that differentiate into long-lived cells in the first week of life via GM-CSF. *J. Exp. Med.* **23**, 1977–1992 (2013).

42. O. Lakhdari, A. Yamamura, G. E. Hernandez, K. K. Anderson, S. J. Lund, G. O. Oppong-Nonterah, H. M. Hoffman, L. S. Prince, Differential immune activation in fetal macrophage populations. *Sci. Rep.* **9**, 7677 (2019).

43. O. J. Mezu-Ndubuisi, A. Maheshwari, Role of macrophages in fetal development and perinatal disorders. *Pediatr. Res.* **90**, 513–523 (2021).

44. N. P. Varghese, R. H. Tillman, R. L. Keller, Pulmonary hypertension is an important co-morbidity in developmental lung diseases of infancy: Bronchopulmonary dysplasia and congenital diaphragmatic hernia. *Pediatr. Pulmonol.* **56**, 670–677 (2021).

45. S. N. Acker, E. W. Mandell, S. Sims-Lucas, J. Gien, S. H. Abman, C. Galambos, Histologic identification of prominent intrapulmonary anastomotic vessels in severe congenital diaphragmatic hernia. *J. Pediatr.* **166**, 178–183 (2015).

46. T. V. Kalymbetova, B. Selvakumar, J. A. Rodríguez-Castillo, M. Gunjak, C. Malainou, M. R. Heindl, A. Moiseenko, C. M. Chao, I. Vadász, K. Mayer, J. Lohmeyer, S. Bellusci, E. Böttcher-Friebertshäuser, W. Seeger, S. Herold, R. E. Morty, Resident alveolar macrophages are master regulators of arrested alveolarization in experimental bronchopulmonary dysplasia. *J. Pathol.* **245**, 153–159 (2018).

47. A. C. Matei, L. Antounians, A. Zani, Extracellular vesicles as a potential therapy for neonatal conditions: State of the art and challenges in clinical translation. *Pharmaceutics* **11**, 404 (2019).

48. E. Delavogia, D. P. Ntentakis, J. A. Cortinas, A. Fernandez-Gonzalez, S. A. Mitsialis, S. Kourembanas, Mesenchymal stromal/stem cell extracellular vesicles and perinatal injury: One formula for many diseases. *Stem Cells* **40**, 991–1007 (2022).

49. K. Khalaj, R. L. Figueira, L. Antounians, G. Lauriti, A. Zani, Systematic review of extracellular vesicle-based treatments for lung injury: Are EVs a potential therapy for COVID-19? *J. Extracell. Vesicles* **9**, 1795365 (2020).

50. E. Zani-Ruttenstock, L. Antounians, K. Khalaj, R. L. Figueira, A. Zani, The role of exosomes in the treatment, prevention, diagnosis, and pathogenesis of COVID-19. *Eur. J. Pediatr. Surg.* **31**, 326–334 (2021).

51. V. Sengupta, S. Sengupta, A. Lazo, P. Woods, A. Nolan, N. Bremer, Exosomes derived from bone marrow mesenchymal stem cells as treatment for severe COVID-19. *Stem Cells Dev.* **29**, 747–754 (2020).

52. F. Pederiva, M. Ghionzoli, A. Pierro, P. De Coppi, J. A. Tovar, Amniotic fluid stem cells rescue both in vitro and in vivo growth, innervation, and motility in nitrofen-exposed hypoplastic rat lungs through paracrine effects. *Cell Transplant.* **22**, 1683–1694 (2013).

53. J. Di Bernardo, M. M. Maiden, M. B. Hershenson, S. M. Kunisaki, Amniotic fluid derived mesenchymal stromal cells augment fetal lung growth in a nitrofen explant model. *J. Pediatr. Surg.* **49**, 859–865 (2014).

54. L. Antounians, A. Tzanetakis, O. Pellerito, V. D. Catania, A. Sulistyo, L. Montalva, M. J. McVey, A. Zani, The regenerative potential of amniotic fluid stem cell extracellular vesicles: Lessons learned by comparing different isolation techniques. *Sci. Rep.* **9**, 1837 (2019).

55. L. Mezzasoma, I. Bellezza, P. Orvietani, G. Manni, M. Gargaro, K Sagini, A. Llorente, P. Scarpelli, L. Pascucci, B. Cellini, V. N. Talesa, F. Fallarino, R. Romani, Amniotic fluid stem cell-derived extracellular vesicles are independent metabolic units capable of modulating inflammasome activation in THP-1 cells. *FASEB J.* **36**, e22218 (2022).

56. B. Li, C. Lee, J. S. O'Connell, L. Antounians, N. Ganji, M. Alganabi, M. Cadete, F. Nascimben, Y. Koike, A. Hock, S. R. Botts, R. Y. Wu, H. Miyake, A. Minich, M. F. Maalouf, E. Zani-Ruttenstock, Y. Chen, K. C. Johnson-Henry, P. De Coppi, S. Eaton, P. Maattanen, P. Delgado Olguin, A. Zani, P. M. Sherman, A. Pierro, Activation of Wnt signaling by amniotic fluid stem cell-derived extracellular vesicles attenuates intestinal injury in experimental necrotizing enterocolitis. *Cell Death Dis.* **11**, 750 (2020).

57. J. S. O'Connell, C. Lee, N. Farhat, L. Antounians, A. Zani, B. Li, A. Pierro, Administration of extracellular vesicles derived from human amniotic fluid stem cells: A new treatment for necrotizing enterocolitis. *Pediatr. Surg. Int.* **37**, 301–309 (2021).

58. M. Hurskainen, I. Mižíková, D. P. Cook, N. Andersson, C. Cyr-Depauw, F. Lesage, E. Helle, L. Renesme, R. P. Jankov, M. Heikinheimo, B. C. Vanderhyden, B. Thébaud, Single cell transcriptomic analysis of murine lung development on hyperoxia-induced damage. *Nat. Commun.* **12**, 1565 (2021).

59. S. Chen, J. Wang, K. Zhang, B. Ma, X. Li, R. Wei, H. Nian, LncRNA Neat1 targets NonO and miR-128-3p to promote antigen-specific Th17 cell responses and autoimmune inflammation. *Cell Death Dis.* **14**, 610 (2023).

60. T. S. Cohen, Role of microRNA in the lung's innate immune response. *J. Innate Immun.* **9**, 243–249 (2017).

61. S. Liu, S. Gao, Z. Yang, P. Zhang, miR-128-3p reduced acute lung injury induced by sepsis via targeting PEL12. *Open Med. (Wars)* **16**, 1109–1120 (2021).

62. H. Schneider, F. Faschingbauer, S. Schuepbach-Mallepell, I. Körber, S. Wohlfart, A. Dick, M. Wahlbuhl, C. Kowalczyk-Quintas, M. Vigolo, N. Kirby, C. Tannert, O. Rompel, W. Rascher, M. W. Beckmann, P. Schneider, Prenatal correction of X-linked hypohidrotic ectodermal dysplasia. *N. Engl. J. Med.* **378**, 1604–1610 (2018).

63. S. Sheller-Miller, K. Choi, C. Choi, R. Menon, Cyclic-recombinase-reporter mouse model to determine exosome communication and function during pregnancy. *Am. J. Obstet. Gynecol.* **221** 502.e1–502.e12 (2019).

64. J. L. Cohen, P. Chakraborty, K. Fung-Kee-Fung, M. E. Schwab, D. Bali, S. P. Young, M. H. Gelb, H. Khaledi, A. DiBattista, S. Smallshaw, F. Moretti, D. Wong, C. Lacroix, D. El Demellawy, K. C. Strickland, J. Lougheed, A. Moon-Grady, B. R. Lianoglou, P. Harmatz, P. S. Kishnani, T. C. MacKenzie, In utero enzyme-replacement therapy for infantile-onset Pompe's disease. *N. Engl. J. Med.* **387**, 2150–2158 (2022).

65. L. Antounians, A. Zani, Beyond the diaphragm and the lung: A multisystem approach to understanding congenital diaphragmatic hernia. *Pediatr. Surg. Int.* **39**, 194 (2023).

66. M. Blundell, F. Doktor, R. L. Figueira, K. Khalaj, G. Biouss, L. Antounians, A. Zani, Anti-inflammatory effects of antenatal administration of stem cell derived extracellular vesicles in the brain of rat fetuses with congenital diaphragmatic hernia. *Pediatr. Surg. Int.* **39**, 291 (2023).

67. C. Théry, K. W. Witwer, E. Aikawa, M. J. Alcaraz, J. D. Anderson, R. Andriantsitohaina, A. Antoniou, T. Arab, F. Archer, G. K. Atkin-Smith, D. C. Ayre, J.-M. Bach, D. Bachurski, H.

Baharvand, L. Balaj, S. Baldacchino, N. N. Bauer, A. A. Baxter, M. Bebawy, C. Beckham, A. B. Zavec, A. Benmoussa, A. C. Berardi, P. Bergese, E. Bielska, C. Blenkiron, S. Bobis-Wozowicz, E. Boilard, W. Boireau, A. Bongiovanni, F. E. Borràs, S. Bosch, C. M. Boulanger, X. Breakefield, A. M. Breglio, M. Á. Brennan, D. R. Brigstock, A. Brisson, M. L. Broekman, J. F. Bromberg, P. Bryl-Górecka, S. Buch, A. H. Buck, D. Burger, S. Busatto, D. Buschmann, B. Bussolati, E. I. Buzás, J. B. Byrd, G. Camussi, D. R. Carter, S. Caruso, L. W. Chamley, Y.-T. Chang, C. Chen, S. Chen, L. Cheng, A. R. Chin, A. Clayton, S. P. Clerici, A. Cocks, E. Cocucci, R. J. Coffey, A. Cordeiro-da-Silva, Y. Couch, F. A. Coumans, B. Coyle, R. Crescitelli, M. F. Criado, C. D'Souza-Schorey, S. Das, A. D. Chaudhuri, P. de Candia, E. F. De Santana, O. D. Wever, H. A. Del Portillo, T. Demaret, S. Deville, A. Devitt, B. Dhondt, D. D. Vizio, L. C. Dieterich, V. Dolo, A. P. D. Rubio, M. Dominici, M. R. Dourado, T. A. Driedonks, F. V. Duarte, H. M. Duncan, R. M. Eichenberger, K. Ekström, S. E. Andaloussi, C. Elie-Caille, U. Erdbrügger, J. M. Falcón-Pérez, F. Fatima, J. E. Fish, M. Flores-Bellver, A. Försönits, A. Frelet-Barrand, F. Fricke, G. Fuhrmann, S. Gabrielsson, A. Gámez-Valero, C. Gardiner, K. Gärtner, R. Gaudin, Y. S. Gho, B. Giebel, C. Gilbert, M. Gimona, I. Giusti, D. C. Goberdhan, A. Görgens, S. M. Gorski, D. W. Greening, J. C. Gross, A. Gualerzi, G. N. Gupta, D. Gustafson, A. Handberg, R. A. Haraszti, P. Harrison, H. Hegyesi, A. Hendrix, A. F. Hill, F. H. Hochberg, K. F. Hoffmann, B. Holder, H. Holthofer, B. Hosseinkhani, G. Hu, Y. Huang, V. Huber, S. Hunt, A. G.-E. Ibrahim, T. Ikezu, J. M. Inal, M. Isin, A. Ivanova, H. K. Jackson, S. Jacobsen, S. M. Jay, M. Jayachandran, G. Jenster, L. Jiang, S. M. Johnson, J. C. Jones, A. Jong, T. Jovanovic-Talisman, S. Jung, R. Kalluri, S.-I. Kano, S. Kaur, Y. Kawamura, E. T. Keller, D. Khamari, E. Khomyakova, A. Khvorova, P. Kierulf, K. P. Kim, T. Kislinger, M. Klingeborn, D. J. Klinke II, M. Kornek, M. M. Kosanović, Á. F. Kovács, E.-M. Krämer-Albers, S. Krasemann, M. Krause, I. V. Kurochkin, G. D. Kusuma, S. Kuypers, S. Laitinen, S. M. Langevin, L. R. Languino, J. Lannigan, C. Lässer, L. C. Laurent, G. Lavieu, E. Lázaro-Ibáñez, S. L. Lay, M.-S. Lee, Y. X. F. Lee, D. S. Lemos, M. Lenassi, A. Leszczynska, I. T. Li, K. Liao, S. F. Libregts, E. Ligeti, R. Lim, S. K. Lim, A. Linē, K. Linnemannstöns, A. Llorente, C. A. Lombard, M. J. Lorenowicz, Á. M. Lörincz, J. Lötvall, J. Lovett, M. C. Lowry, X. Loyer, Q. Lu, B. Lukomska, T. R. Lunavat, S. L. Maas, H. Malhi, A. Marcilla, J. Mariani, J. Mariscal, E. S. Martens-Uzunova, L. Martin-Jaular, M. C. Martinez, V. R. Martins, M. Mathieu, S. Mathivanan, M. Maugeri, L. K. McGinnis, M. J. McVey, D. G. Meckes Jr., K. L. Meehan, I. Mertens, V. R. Minciacchi, A. Möller, M. M.

Jørgensen, A. Morales-Kastresana, J. Morhayim, F. Mullier, M. Muraca, L. Musante, V. Mussack, D. C. Muth, K. H. Myburgh, T. Najrana, M. Nawaz, I. Nazarenko, P. Nejsum, C. Neri, T. Neri, R. Nieuwland, L. Nimrichter, J. P. Nolan, E. N. N. Hoen, N. N. Hooten, L. O'Driscoll, T. O'Grady, A. O'Loghlen, T. Ochiya, M. Olivier, A. Ortiz, L. A. Ortiz, X. Osteikoetxea, O. Østergaard, M. Ostrowski, J. Park, D. M. Pegtel, H. Peinado, F. Perut, M. W. Pfaffl, D. G. Phinney, B. C. Pieters, R. C. Pink, D. S. Pisetsky, E. P. von Strandmann, I. Polakovicova, I. K. Poon, B. H. Powell, I. Prada, L. Pulliam, P. Quesenberry, A. Radeghieri, R. L. Raffai, S. Raimondo, J. Rak, M. I. Ramirez, G. Raposo, M. S. Rayyan, N. Regev-Rudzki, F. L. Ricklefs, P. D. Robbins, D. D. Roberts, S. C. Rodrigues, E. Rohde, S. Rome, K. M. Rouschop, A. Rughetti, A. E. Russell, P. Saá, S. Sahoo, E. Salas-Huenuleo, C. Sánchez, J. A. Saugstad, M. J. Saul, R. M. Schiffelers, R. Schneider, T. H. Schøyen, A. Scott, E. Shahaj, S. Sharma, O. Shatnyeva, F. Shekari, G. V. Shelke, A. K. Shetty, K. Shiba, P. R.-M. Siljander, A. M. Silva, A. Skowronek, O. L. Snyder 2nd, R. P. Soares, B. W. Sódar, C. Soekmadji, J. Sotillo, P. D. Stahl, W. Stoorvogel, S. L. Stott, E. F. Strasser, S. Swift, H. Tahara, M. Tewari, K. Timms, S. Tiwari, R. Tixeira, M. Tkach, W. S. Toh, R. Tomasini, A. C. Torrecilhas, J. P. Tosar, V. Toxavidis, L. Urbanelli, P. Vader, B. W. van Balkom, S. G. van der Grein, J. Van Deun, M. J. van Herwijnen, K. V. Keuren-Jensen, G. van Niel, M. E. van Royen, A. J. van Wijnen, M. H. Vasconcelos, I. J. Vechetti Jr., T. D. Veit, L. J. Vella, É. Velot, F. J. Verweij, B. Vestad, J. L. Viñas, T. Visnovitz, K. V. Vukman, J. Wahlgren, D. C. Watson, M. H. Wauben, A. Weaver, J. P. Webber, V. Weber, A. M. Wehman, D. J. Weiss, J. A. Welsh, S. Wendt, A. M. Wheelock, Z. Wiener, L. Witte, J. Wolfram, A. Xagorari, P. Xander, J. Xu, X. Yan, M. Yáñez-Mó, H. Yin, Y. Yuana, V. Zappulli, J. Zarubova, V. Žėkas, J.-Y. Zhang, Z. Zhao, L. Zheng, A. R. Zheutlin, A. M. Zickler, P. Zimmermann, A. M. Zivkovic, D. Zocco, E. K. Zuba-Surma, Minimal information for studies of extracellular vesicles 2018 (MISEV2018): A position statement of the International Society for Extracellular Vesicles and update of the MISEV2014 guidelines. *J. Extracell. Vesicles* **7**, 1535750 (2018).

68. L. Antounians, R. L. Figueira, L. Sbragia, A. Zani, Congenital diaphragmatic hernia: State of the art in translating experimental research to the bedside. *Eur. J. Pediatr. Surg.* **29**, 317–327 (2019).

69. L. Montalva, L. Antounians, A. Zani, Pulmonary hypertension secondary to congenital diaphragmatic hernia: Factors and pathways involved in pulmonary vascular remodeling. *Pediatr. Res.* **85**, 754–768 (2019).

70. I. Iritani, Experimental study on embryogenesis of congenital diaphragmatic hernia. *Anat. Embryol. (Berl.)* **169**, 133–139 (1984).

71. C. Kekik, S. K. Besisik, Y. Seyhun, F. S. Oguz, D. Sargin, M. N. Carin, Relationship between HLA tissue type, CMV infection, and acute graft-vs-host disease after allogeneic hematopoietic stem cell transplantation: Single-center experience. *Transplant. Proc.* **41**, 3859–3862 (2009).

72. S. Takayama, K. Sakai, S. Fumino, T. Furukawa, T. Kishida, O. Mazda, T. Tajiri, An intra-amniotic injection of mesenchymal stem cells promotes lung maturity in a rat congenital diaphragmatic hernia model. *Pediatr. Surg. Int.* **35**, 1353–1361 (2019).

73. S. T. Somashekar, I. Sammour, J. Huang, J. Dominguez-Bendala, R. Pastori, S. Alvarez-Cubela, E. Torres, S. Wu, K. C. Young, Intra-amniotic soluble endoglin impairs lung development in neonatal rats. *Am. J. Respir. Cell Mol. Biol.* **57**, 468–476 (2017).

74. K. Kobayashi, R. P. Lemke, J. J. Greer, Ultrasound measurements of fetal breathing movements in the rat. *J. Appl. Physiol.* **91**, 316–320 (1985).

75. C. Hsia, D. M. Hyde, M. Ochs, E. R. Weibel, ATS/ERS Joint Task Force on Quantitative Assessment of Lung Structure, An official research policy statement of the American Thoracic Society/European Respiratory Society: Standards for quantitative assessment of lung structure. *Am. J. Respir. Crit. Care Med.* **181**, 394–418 (2010).

76. S. Jin, C. F. Guerrero-Juarez, L. Zhang, I. Chang, R. Ramos, C. H. Kuan, P. Myung, M. V. Plikus, Q. Nie, Inference and analysis of cell-cell communication using CellChat. *Nat. Commun.* **12**, 1088 (2021).

77. J. Reimand, M. Kull, H. Peterson, J. Hansen, J. Vilo, g:Profiler—A web-based toolset for functional profiling of gene lists from large-scale experiments. *Nucleic Acids Res.* **35**, W193–200 (2007).

78. M. Gillespie, B. Jassal, R. Stephan, M. Milacic, K. Rothfels, A. Senff-Ribeiro, J. Griss, C. Sevilla, L. Matthews, C. Gong, C. Deng, T. Varusai, E. Ragueneau, Y. Haider, B. May, V. Shamovsky, J. Weiser, T. Brunson, N. Sanati, L. Beckman, X. Shao, A. Fabregat, K. Sidiropoulos, J. Murillo, G. Viteri, J. Cook, S. Shorser, G. Bader, E. Demir, C. Sander, R. Haw, G. Wu, L. Stein, H. Hermjakob, P. D'Eustachio, The reactome pathway knowledgebase 2022. *Nucleic Acids Res.* **50**, D687-D692 (2022).

79. J. Alquicira-Hernandez, A. Sathe, H. P. Ji, Q. Nguyen, J. E. Powell, scPred: Accurate supervised method for cell-type classification from single-cell RNA-seq data. *Genome Biol.* **20**, 264–281 (2019).

80. J. Hong, D. Arneson, S. Umar, G. Ruffenach, C. M. Cunningham, I. S. Ahn, G. Diamante, M. Bhetraratana, J. F. Park, E. Said, C. Huynh, T. Le, L. Medzikovic, M. Humbert, F. Soubrier, D. Montani, B. Girerd, D. A. Trégouët, R. Channick, R. Saggar, M. Eghbali, X. Yang, Single-cell study of two rat models of pulmonary arterial hypertension reveals connections to human pathobiology and drug repositioning. *Am. J. Respir. Crit. Care Med.* **203**, 1006–1022 (2021).

81. M. Herrera-Rivero, R. Zhang, S. Heilmann-Heimbach, A. Mueller, S. Bagci, T. Dresbach, L. Schröder, S. Holdenrieder, H. M. Reutter, F. Kipfmueller, Circulating microRNAs are associated with pulmonary hypertension and development of chronic lung disease in congenital diaphragmatic hernia. *Sci. Rep.* **8**, 10735 (2018).

82. F. Piersigilli, M. Syed, T. T. Lam, A. Dotta, M. Massoud, P. Vernocchi, A. Quagliariello, L. Putignani, C. Auriti, G. Salvatori, P. Bagolan, V. Bhandari, An omic approach to congenital diaphragmatic hernia: A pilot study of genomic, microRNA, and metabolomic profiling. *J. Perinatol.* **40**, 952–961 (2020).

83. N. Khoshgoo, R. Visser, L. Falk, C. A. Day, D. Ameis, B. M. Iwasiow, F. Zhu, A. Öztürk, S. Basu, M. Pind, A. Fresnosa, M. Jackson, V. K. Siragam, G. Stelmack, G. G. Hicks, A. J. Halayko, R. Keijzer, MicroRNA-200b regulates distal airway development by maintaining epithelial integrity. *Sci. Rep.* **7**, 6382 (2017).

84. M. P. Eastwood, J. Deprest, F. M. Russo, H. Wang, D. Mulhall, B. Iwasiow, T. H. Mahood, R. Keijzer, MicroRNA 200b is upregulated in the lungs of fetal rabbits with surgically induced diaphragmatic hernia. *Prenat. Diagn.* **38**, 645–653 (2018).

85. M. Mudri, S. A. Smith, C. Vanderboor, J. Davidson, T. R. H. Regnault, A. Bütter, The effects of tracheal occlusion on Wnt signaling in a rabbit model of congenital diaphragmatic hernia. *J. Pediatr. Surg.* **54**, 937–944 (2019).

86. E. L. Sanford, K. W. Choy, P. K. Donahoe, A. A. Tracy, R. Hila, M. Loscertales, M. Longoni, MiR-449a affects epithelial proliferation during the pseudoglandular and canalicular phases of avian and mammal lung development. *PLOS ONE* **11**, e0149425 (2016).

87. S. Zhu, Q. He, R. Zhang, Y. Wang, W. Zhong, H. Xia, J. Yu, Decreased expression of miR-33 in fetal lungs of nitrofen-induced congenital diaphragmatic hernia rat model. *J. Pediatr. Surg.* **51**, 1096–1100 (2016).

88. D. Mulhall, N. Khoshgoo, R. Visser, B. Iwasiow, C. Day, F. Zhu, P. Eastwood, R. Keijzer, miR-200 family expression during normal and abnormal lung development due to congenital diaphragmatic hernia at the later embryonic stage in the nitrofen rat model. *Pediatr. Surg. Int.* **36**, 1429–1436 (2020).

89. N. Khoshgoo, R. Kholdebarin, P. Pereira-Terra, T. H. Mahood, L. Falk, C. A. Day, B. M. Iwasiow, F. Zhu, D. Mulhall, C. Fraser, J. Correia-Pinto, R. Keijzer, Prenatal microRNA miR-200b therapy improves nitrofen-induced pulmonary hypoplasia associated with congenital diaphragmatic hernia. *Ann. Surg.* **269**, 979–987 (2019).

90. T. H. Mahood, D. R. Johar, B. M. Iwasiow, W. Xu, R. Keijzer, The transcriptome of nitrofen-induced pulmonary hypoplasia in the rat model of congenital diaphragmatic hernia. *Pediatr. Res.* **79**, 766–775 (2016).

91. X. Li, H. Liu, Y. Lv, W. Yu, X. Liu, C. Liu, MiR-130a-5p/Foxa2 axis modulates fetal lung development in congenital diaphragmatic hernia by activating the Shh/Gli1 signaling pathway. *Life Sci.* **241**, 117166 (2020).

92. Y. Ru, K. J. Kechris, B. Tabakoff, P. Hoffman, R. A. Radcliffe, R. Bowler, S. Mahaffey, S. Rossi, G. A. Calin, L. Bemis, D. Theodorescu, The multiMiR R package and database: Integration of microRNA-target interactions along with their disease and drug associations. *Nucleic Acids Res.* **42**, e133 (2014).

93. P. Shannon, A. Markiel, O. Ozier, N. S. Baliga, J. T. Wang, D. Ramage, N. Amin, B. Schwikowski, T. Ideker, Cytoscape: A software environment for integrated models of biomolecular interaction networks. *Genome Res.* **13**, 2498–2504 (2003).

94. Z. Li, X. Gong, D. Li, X. Yang, Q. Shi, X. Ju, Intratracheal transplantation of amnion-derived mesenchymal stem cells ameliorates hyperoxia-induced neonatal hyperoxic lung injury via aminoacyl-peptide hydrolase. *Int. J. Stem. Cells.* **13**, 221–236 (2020).

95. G. R. Willis, A. Fernandez-Gonzalez, M. Reis, V. Yeung, X. Liu, M. Ericsson, N. A. Andrews, S. A. Mitsialis, S. Kourembanas, Mesenchymal stromal cell-derived small extracellular vesicles restore lung architecture and improve exercise capacity in a model of neonatal hyperoxia-induced lung injury. *J. Extracell. Vesicles* **9**, 1790874 (2020).

96. A. Porzionato, P. Zaramella, A. Dedja, D. Guidolin, K. Van Wemmel, V. Macchi, M. Jurga, G. Perilongo, R. De Caro, E. Baraldi, M. Muraca, Intratracheal administration of clinical-grade mesenchymal stem cell-derived extracellular vesicles reduces lung injury in a rat model of bronchopulmonary dysplasia. *Am. J. Physiol. Lung Cell. Mol. Physiol.* **316**, L6-L19 (2019).

97. R. K. Braun, C. Chetty, V. Balasubramaniam, R. Centanni, K. Haraldsdottir, P. Hematti, M. W. Eldridge, Intraperitoneal injection of MSC-derived exosomes prevent experimental bronchopulmonary dysplasia. *Biochem. Biophys. Res. Commun.* **503**, 2653–2658 (2018).

98. S. Chaubey, S. Thueson, D. Ponnalagu, M. A. Alam, C. P. Gheorghe, Z. Aghai, H. Singh, V. Bhandari. Early gestational mesenchymal stem cell secretome attenuates experimental bronchopulmonary dysplasia in part via exosome-associated factor TSG-6. *Stem Cell Res. Ther.* **9**, 173 (2018).

99. G. R. Willis, A. Fernandez-Gonzalez, J. Anastas, S. H. Vitali, X. Liu, M. Ericsson, A. Kwong, S. A. Mitsialis, S. Kourembanas, Mesenchymal stromal cell exosomes ameliorate experimental bronchopulmonary dysplasia and restore lung function through macrophage immunomodulation. *Am. J. Respir. Crit. Care Med.* **197**, 104–116 (2018).

100. S. Y. Ahn, W. S. Park, Y. E. Kim, D. K. Sung, S. I. Sung, J. Y. Ahn, Y. S. Chang, MSK1 functions as a transcriptional coactivator of p53 in the regulation of p21 gene expression. *Exp. Mol. Med.* **50**, 1–12 (2018).

101. A. Tieu, K. Hu, C. Gnyra, J. Montroy, D. A. Fergusson, D. S. Allan, D. J. Stewart, B. Thébaud, M. M. Lalu, Mesenchymal stromal cell extracellular vesicles as therapy for acute and chronic respiratory diseases: A meta-analysis. *J. Extracell. Vesicles* **10**, e12141 (2021).

102. G. R. Willis, M. Reis, A. H. Gheinani, A. Fernandez-Gonzalez, E. S. Taglauer, V. Yeung, X. Liu, M. Ericsson, E. Haas, S. A. Mitsialis, S. Kourembanas, Extracellular vesicles protect the neonatal lung from hyperoxic injury through the epigenetic and transcriptomic reprogramming of myeloid cells. *Am. J. Respir. Crit. Care Med.* **204**, 1418–1432 (2021).

103. S. Q. Ye, B. A. Simon, J. P. Maloney, A. Zambelli-Weiner, L. Gao, A. Grant, R. B. Easley, B. J. McVerry, R. M. Tuder, T. Standiford, R. G. Brower, K. C. Barnes, J. G. Garcia, Pre-B-cell colony-enhancing factor as a potential novel biomarker in acute lung injury. *Am. J. Respir. Crit. Care Med.* **171**, 361–370 (2005).

104. K. A. Lee, M. N. Gong, Pre-B-cell colony-enhancing factor and its clinical correlates with acute lung injury and sepsis. *Chest* **140**, 382–390 (2011).

105. A. Matsuda, W. L. Yang, A. Jacob, M. Aziz, S. Matsuo, T. Matsutani, E. Uchida, P. Wang, FK866, a visfatin inhibitor, protects against acute lung injury after intestinal ischemia-reperfusion in mice via NF-κB pathway. *Ann. Surg.* **259**, 1007–1017 (2014).

106. M. Ochman, M. Maruszewski, J. Wojarski, S. Żegleń, W. Karolak, A. Stanjek-Cichoracka, P. Przybyłowski, M. Zembala, M. Kukla, Serum levels of visfatin, omentin and irisin in patients

with end-stage lung disease before and after lung transplantation. *Ann. Transplant.* **22**, 761–768 (2017).

107. T. Weng, L. Liu, The role of pleiotrophin and beta-catenin in fetal lung development. *Respir. Res.* **11**, 80 (2010).

108. H. A. Himburg, J. R. Harris, T. Ito, P. Daher, J. L. Russell, M. Quarmyne, P. L. Doan, K. Helms, M. Nakamura, E. Fixsen, G. Herradon, T. Reya, N. J. Chao, S. Harroch, J. P. Chute, Pleiotrophin regulates the retention and self-renewal of hematopoietic stem cells in the bone marrow vascular niche. *Cell Rep.* **2**, 964–975 (2012).

109. S. Guardado, D. Ojeda-Juárez, M. Kaul, T. M. Nordgren, Comprehensive review of lipocalin 2-mediated effects in lung inflammation. *Am. J. Physiol. Lung Cell. Mol. Physiol.* **321**, L726-L733 (2021).

110. K. Bry, J. A. Whitsett, U. Lappalainen, IL-1beta disrupts postnatal lung morphogenesis in the mouse. *Am. J. Respir. Cell Mol. Biol.* **36**, 32–42 (2007).

111. A. N. Stouch, A. M. McCoy, R. M. Greer, O. Lakhdari, F. E. Yull, T. S. Blackwell, H. M. Hoffman, L. S. Prince, IL-1β and inflammasome activity link inflammation to abnormal fetal airway development. *J. Immunol.* **196**, 3411–3420 (2016).

112. S. Fernandez-Sauze, C. Delfino, K. Mabrouk, C. Dussert, O. Chinot, P. M. Martin, F. Grisoli, L. Ouafik, F. Boudouresque, Effects of adrenomedullin on endothelial cells in the multistep process of angiogenesis: Involvement of CRLR/RAMP2 and CRLR/RAMP3 receptors. *Int. J. Cancer* **108**, 797–804 (2004).

113. S. Zhang, A. Patel, B. Moorthy, B. Shivanna, Adrenomedullin deficiency potentiates hyperoxic injury in fetal human pulmonary microvascular endothelial cells. *Biochem. Biophys. Res. Commun.* **464**, 1048–1053 (2015).

114. A. Vadivel, S. Abozaid, T. van Haaften, M. Sawicka, F. Eaton, M. Chen, B. Thébaud, Adrenomedullin promotes lung angiogenesis, alveolar development, and repair. *Am. J. Respir. Cell Mol. Biol.* **43**, 152–160 (2010).

115. T. Suzuki, S. Suzuki, N. Fujino, C. Ota, M. Yamada, T. Suzuki, M. Yamaya, T. Kondo, H. Kubo, c-Kit immunoexpression delineates a putative endothelial progenitor cell population in developing human lungs. *Am. J. Physiol. Lung Cell. Mol. Physiol.* **306**, L855–865 (2014).

116. J. Y. Lindsey, K. Ganguly, D. M. Brass, Z. Li, E. N. Potts, S. Degan, H. Chen, B. Brockway, S. N. Abraham, A. Berndt, B. R. Stripp, W. M. Foster, G. D. Leikauf, H. Schulz, J. W. Hollingsworth, c-Kit is essential for alveolar maintenance and protection from emphysema-like disease in mice. *Am. J. Respir. Crit. Care Med.* **183**, 1644–1652 (2011).

117. R. Epaud, F. Aubey, J. Xu, Z. Chaker, M. Clemessy, A. Dautin, K. Ahamed, M. Bonora, N. Hoyeau, J. F. Fléjou, A. Mailleux, A. Clement, A. Henrion-Caude, M. Holzenberger, Knockout of insulin-like growth factor-1 receptor impairs distal lung morphogenesis. *PLOS ONE* **7**, e48071 (2012).

118. H. He, J. Snowball, F. Sun, C. L. Na, J. A. Whitsett, IGF1R controls mechanosignaling in myofibroblasts required for pulmonary alveologenesis. *JCI Insight* **6**, 144863 (2021).

119. J. Baker, J. P. Liu, E. J. Robertson, A. Efstratiadis, Role of insulin-like growth factors in embryonic and postnatal growth. *Cell* **75**, 73–82 (1993).

120. H. Liu, L. Chang, Z. Rong, H. Zhu, Q. Zhang, H. Chen, W. Li, Association of insulin-like growth factors with lung development in neonatal rats. *J. Huazhong Univ. Sci. Technol. Med. Sci.* **24**, 162–165 (2004).

121. E. Ruttenstock, T. Doi, J. Dingemann, P. Puri, Insulinlike growth factor receptor type 1 and type 2 are downregulated in the nitrofen-induced hypoplastic lung. *J. Pediatr. Surg.* **45**, 1349–1353 (2010).

122. M. Jeansson, A. Gawlik, G. Anderson, C. Li, D. Kerjaschki, M. Henkelman, S. E. Quaggin, Angiopoietin-1 is essential in mouse vasculature during development and in response to injury. *J. Clin. Invest.* **121**, 2278–2289 (2011).

123. N. Ferrara, Vascular endothelial growth factor: Basic science and clinical progress. *Endocr. Rev.* **25**, 581–611 (2004).

124. M. R. Chinoy, M. M. Graybill, S. A. Miller, C. M. Lang, G. L. Kauffman, Angiopoietin-1 and VEGF in vascular development and angiogenesis in hypoplastic lungs. *Am. J. Physiol. Lung Cell. Mol. Physiol.* **283**, L60–66 (2002).

125. K. Miura da Costa, A. T. Fabro, C. Becari, R. L. Figueira, A. F. Schmidt, R. Ruano, L. Sbragia, Honeymoon period in newborn rats with CDH is associated with changes in the VEGF signaling pathway. *Front. Pediatr.* **9**, 698217 (2021).

126. L. L. Abler, S. L. Mansour, X. Sun, Conditional gene inactivation reveals roles for Fgf10 and Fgfr2 in establishing a normal pattern of epithelial branching in the mouse lung. *Dev. Dyn.* **238**, 1999–2013 (2009).

127. Y. Yin, D. M. Ornitz, FGF9 and FGF10 activate distinct signaling pathways to direct lung epithelial specification and branching. *Sci. Signal.* **13**, eaay4353 (2020).

128. S. Danopoulos, J. Shiosaki, D. Al Alam, FGF signaling in lung development and disease: Human versus mouse. *Front. Genet.* **10**, 170 (2019).

129. S. Danopoulos, M. E. Thornton, B. H. Grubbs, M. R. Frey, D. Warburton, S. Bellusci, D. Al Alam, Discordant roles for FGF ligands in lung branching morphogenesis between human and mouse. *J. Pathol.* **247**, 254–265 (2019).

130. J. M. Klein, B. L. Fritz, T. A. McCarthy, C. L. Wohlford-Lenane, J. M. Snyder, Localization of epidermal growth factor receptor in alveolar epithelium during human fetal lung development in vitro. *Exp. Lung Res.* **21**, 917–939 (1995).

131. J. Li, T. Hu, W. Liu, B. Xiang, X. Jiang, Effect of epidermal growth factor on pulmonary hypoplasia in experimental diaphragmatic hernia. *J. Pediatr. Surg.* **39**, 37–42 (2004).

132. C. K. Peng, C. P. Wu, J. Y. Lin, S. C. Peng, C. H. Lee, K. L. Huang, C. H. Shen, Gas6/Axl signaling attenuates alveolar inflammation in ischemia-reperfusion-induced acute lung injury by up-regulating SOCS3-mediated pathway. *PLOS ONE* **14**, e0219788 (2019).

133. Q. Wu, X. Zhou, Y. Wang, Y. Hu, LncRNA GAS5 promotes spermidine-induced autophagy through the miRNA-31-5p/NAT8L axis in pulmonary artery endothelial cells of patients with CTEPH. *Mol. Med. Rep.* **26**, 297 (2022).

134. M. J. Heeb, Role of the PROS1 gene in thrombosis: Lessons and controversies. *Expert Rev. Hematol.* **1**, 9–12 (2008).

135. L. Suleiman, Y. Muataz, C. Négrier, H. Boukerche, Protein S-mediated signal transduction pathway regulates lung cancer cell proliferation, migration and angiogenesis. *Hematol. Oncol. Stem Cell Ther.* **1**, S1658–3876 (2021).

136. M. Kagoshima, T. Ito, Diverse gene expression and function of semaphorins in developing lung: Positive and negative regulatory roles of semaphorins in lung branching morphogenesis. *Genes Cells* **6**, 559–571 (2001).

137. C. E. Dammann, H. C. Nielsen, K. L. Carraway III, Role of neuregulin-1β in the developing lung. *Am. J. Respir. Crit. Care Med.* **167**, 1711–1716 (2003).

138. J. Liu, D. Nethery, J. A. Kern, Neuregulin-1 induces branching morphogenesis in the developing lung through a P13K signal pathway. *Exp. Lung Res.* **30**, 465–478 (2004).

139. O. Boucherat, A. Benachi, B. Chailley-Heu, M. L. Franco-Montoya, C. Elie, J. Martinovic, J. R. Bourbon, Surfactant maturation is not delayed in human fetuses with diaphragmatic hernia. *PLoS Med.* **4**, e237 (2007).

140. C. V. Jones, M. A. Alikhan, M. O'Reilly, F. Sozo, T. M. Williams, R. Harding, G. Jenkin, S. D. Ricardo, The effect of CSF-1 administration on lung maturation in a mouse model of neonatal hyperoxia exposure. *Respir. Res.* **15**, 110 (2014).